International Journal of Power Electronics and Drive System (IJPEDS)
Vol. 8, No. 3, September 2017, pp. 1070~1079
ISSN: 2088-8694, DOI: 10.11591/ijpeds.v8i3.pp1070-1079

Improvement of Torque Capability of Direct Torque Control of Induction Machines

Auzani Jidin[1], New Lai Sim[2], Tole Sutikno[3]
[1,2] Faculty of Electrical Engineering, Universiti Teknikal Malaysia Melaka (UTeM), Malacca, Malaysia
[3]Department of Electrical Engineering, Universitas Ahmad Dahlan (UAD), Yogyakarta, Indoneisia

Article Info

Article history:

Received May 26, 2017
Revised Jul 23, 2017
Accepted Aug 12, 2017

Keyword:

Constant torque region
Direct torque control
Hysteresis based
Induction machine
Overmodulation

ABSTRACT

A control strategy for overmodulation operation of direct torque control hysteresis based in induction machine is proposed. The strategy is to extend the constant torque region as well as to improve the torque capability. The proposed overmodulation strategy is different to SVM based system where the reference stator voltage is available. In order for DTC hysteresis based system to be able to achieve that, several modifications have been applied so that the proposed overmodulation can be achieved by gradually transforming the PWM voltage waveform to six-step mode. Simulated results were provided to demonstrate the effectiveness of the strategy.

Corresponding Author:

Auzani Jidin,
Faculty of Electrical Engineering,
Universiti Teknikal Malaysia Melaka (UTeM),
Malacca, Malaysia.
Email: auzani@utem.edu.my

1. INTRODUCTION

The availability of constant power is very important in applications such as in vehicle drive. In induction machine, various combinations of stator voltage, current and speed is used to estimate the flux and torque. The control of Direct Torque Control (DTC) of induction machines is based on selecting proper voltage vectors to maintain torque and stator flux within the hysteresis band [1]. In [2], voltage vector selection strategy that uses switching table is widely used because of the easy to understand concept a simple implementation. The drawback of a conventional DTC is that the switching frequency is unpredictable according to the machine parameters and speed condition. The system performance will degrade in a certain operating region such as at the low speed region.

In [3], a common approach, space vector modulation (SVM) is used to exploit the overmodulation region in DTC. This strategy manages to obtain maximum torque output in field weakening region. This strategy requires voltage reference to define the mode of overmodulation in SVM. However, DTC hysteresis based is not capable to operate in overmodulation to complete six-step mode.

This paper presents a strategy to extend the constant torque region and improve the torque capability of DTC hysteresis based without ruining the simplicity of basic DTC-hysteresis based structure. This proposed strategy introduces overmodulation strategy by gradually transforming the PWM voltage waveform to six-step mode. The method is different from SVM based system where the reference stator voltage is available and the overmodulation is achieved by modifying the reference voltage.

2. PRINCIPAL OF DIRECT TORQUE CONTROL

2.1. 3-Phase Voltage Source Inverter

Three-phase VSIs cover the medium to high-power applications. The main purpose of these topologies is to provide a three-phase voltage source, where the amplitude, phase, and frequency of the voltages should always be controllable. The standard three-phase VSI topology is as shown below.

In this configuration, the upper switch and lower switch which should not be conducted at the same time [4]. This yield eight possible configurations of six switching devices for S_a^+, S_b^+ and S_c^+ are the switching function of each leg of the inverter. When S_a^+, S_b^+ or S_c^+ equals to 1, it shows that the upper switch is ON while 0 means the lower switch is ON. Figure 2 shows that there are six non-zero voltage vectors and two zero voltage vectors which are located at the origin. The voltage vector is given by [5];

$$\bar{v}_{sk,n} = \frac{2}{3} V_{DC}(S_a^+ + aS_b^+ + a^2 S_c^+) \quad (1)$$

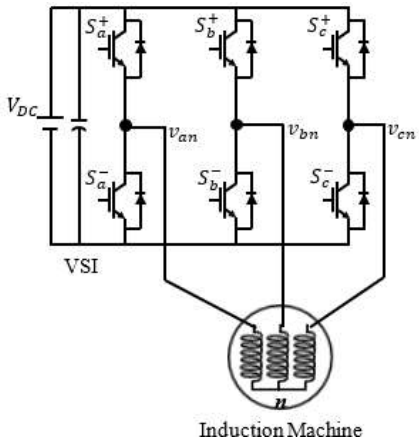

Figure 1. Schematic Diagram of VSI

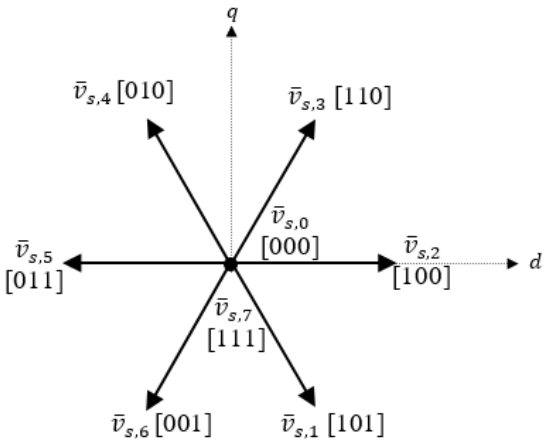

Figure 2. Voltage Space Vectors of a Three-phase Inverter with the Corresponded Switching States

2.2. Direct Flux Control

If the voltage drop across the stator resistance is neglected and over a small period of time the equations can be written in stationary reference frame as below:

$$\Delta\bar{\varphi}_s \equiv \bar{v}_{s,k}.\Delta t \quad (2)$$

In order to select the appropriate voltage vector, the stator flux orientation or position must be known. The stator flux plane is divided into six sectors [6]. Each sector will have a different set of voltage vectors to increase or decrease the flux. When the stator flux touches its upper or lower hysteresis band, a suitable voltage vector is selected to reduce (voltage vector highlighted in black) or increase (voltage vector highlighted in grey) it respectively as illustrated in Figure 3.

In DTC the stator flux is forced to follow a circular locus by limiting its magnitude within the hysteresis band. Figure 4 illustrates that if the stator flux is located in sector I, the voltage vector $\bar{v}_{s,2}$and $\bar{v}_{s,3}$will be selected to increase or decrease the stator flux. If the stator flux falls in sector II, the voltage vector $\bar{v}_{s,3}$ and $\bar{v}_{s,4}$ will be selected to control the stator flux. However, the use of voltage vectors that will results in a very fast decrease or increase in stator flux is usually avoided [7]. This voltage vector selection is to control the stator flux remains within its hysteresis band by using a 2-level hysteresis comparator.

A block diagram of 2-level stator flux hysteresis comparator is shown in Figure 5(a). The estimated flux is subtracted from reference flux to obtain the flux error before fed to the hysteresis comparator. The output of the flux hysteresis comparator is the flux error status. In Figure 5(b), it shows that when estimated flux touches the lower band and flux error touches the upper band, the flux error status produced is "1". When flux error status is "1", it calls for increase in flux. When estimated flux touches the upper band and flux error touches the lower band, the flux error status produced is "0". When flux error status is "0", it calls for decrease in flux. Suitable voltage vector should be selected [8].

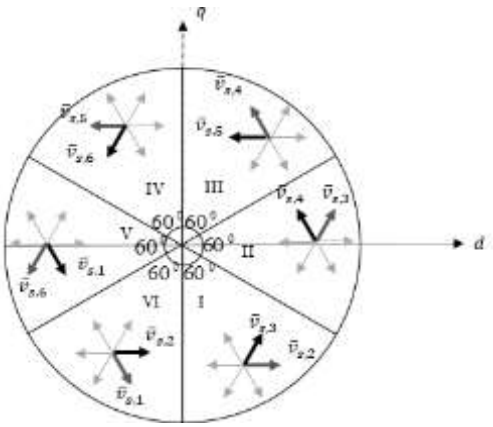

Figure 3. Six Sector of Stator Flux plane

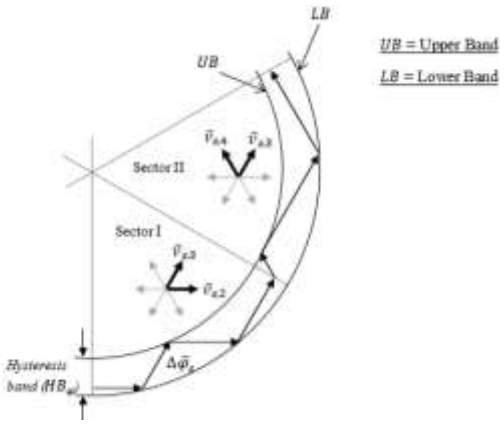

Figure 4. Voltage Vectors Selection Within Hysteresis Band

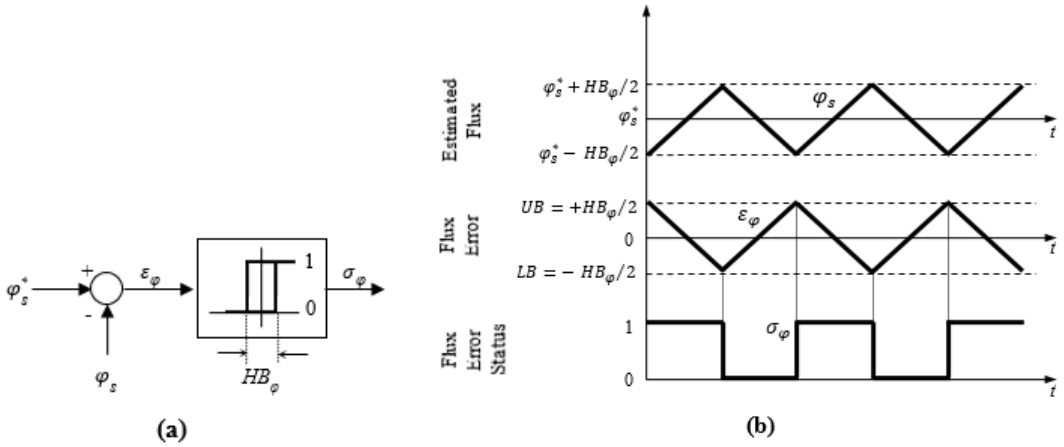

Figure 5. Control of Stator Flux (a) Two-Level Hysteresis Comparator (b) Typical Waveforms

2.4. Direct Torque Control

The principle of torque control can be easily explained by using torque equation in terms of rotor flux and stator flux vectors:

$$T_e = \frac{3}{2} P \frac{L_m}{\sigma L_s L_r} (\varphi_r)(\varphi_s) \sin\delta_{sr} \quad (3)$$

In DTC, the torque is controlled within its hysteresis band similar to the stator flux. The only difference is that DTC uses a three-level hysteresis controller as shown in Figure 6(a). Waveforms of the torque, torque error, speed and torque error status with both positive and negative torque command are shown in Figure 6(b).

The difference between reference and estimated torque gives the error which by restricting it, the control of torque can be accomplished. The comparator will output a torque error status which will produce three level outputs such as -1, 0 or +1 as given in (4). This is similar to the flux status error, the torque error status is used to index the look-up table for selecting suitable voltage vectors.

$$\sigma_T = \begin{cases} +1 & \text{increase torque, error touches } UB \\ 0 & \text{decrease flux, error touches } MB \\ -1 & \text{rapidly decrease torque, error touches } LB \end{cases} \quad (4)$$

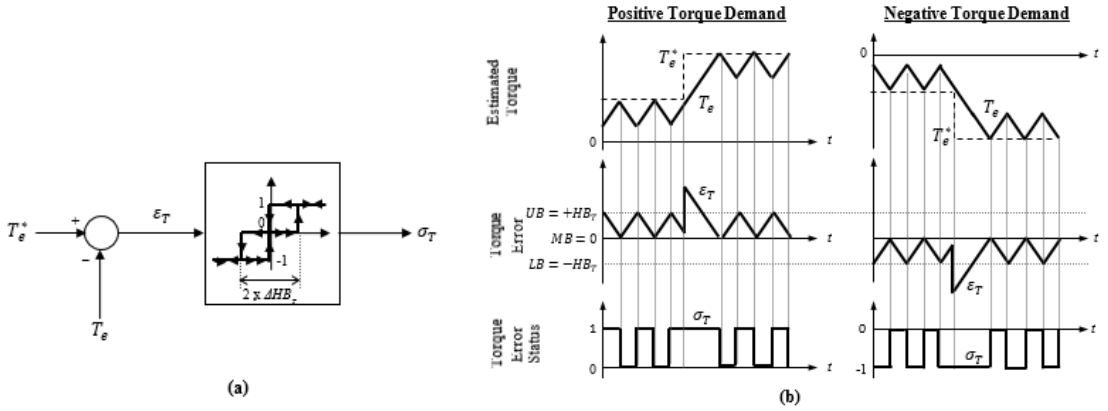

Figure 6. Control of Torque (a) Three-Level Hysteresis Comparator (b) Typical Waveforms for Controlling Positive and Negative Torque

2.5. Switching Stator Selector

By selecting voltage vectors to satisfy the torque and stator flux demand, a decoupled control of flux and torque is achieved. If the stator flux lies in sector k with the motor rotating in counter clockwise, to increase the stator flux and torque, active voltage vector is used. The two zero voltage vectors are used to reduce the torque and stop the stator flux.

Next, reverse voltage vector, $\bar{v}_{s,k-2}$ is used to decrease the torque and flux in forward braking mode. While $\bar{v}_{s,k-1}$ will reduce the torque and increase the flux. A selection table is constructed as shown in Table 1. The table is the combination of torque and stator flux error status and sector in which stator flux occupies [9].

Table 1. Selection Table for Voltage Vector

Stator Flux Error Status	Torque Error Status	Sector 1	Sector 2	Sector 3	Sector 4	Sector 5	Sector 6
1	1	100	110	010	011	001	101
	0	000	111	000	111	000	111
	-1	001	101	100	110	010	011
0	1	110	010	011	001	101	100
	0	111	000	111	000	111	000
	-1	011	001	101	100	110	101

3. PROPOSED STRATEGY

3.1. Optimal Switching Voltage Vectors

The identification of the optimized voltage vector between the two possible voltages vectors depends on the flux position. The sector, k is divided into subsector I and subsector II. The α_k in (5) is the angle within sector for $0 \leq \alpha_k < \frac{\pi}{3}$ rad.

$$0 \leq \alpha_k < \frac{\pi}{6} \text{ rad; subsector I}$$
$$\frac{\pi}{6} \leq \alpha_k < \frac{\pi}{3} \text{ rad; subsector II} \quad (5)$$

Only one active voltage vector is selected instead of regulating the flux by selecting two possible active voltage vectors alternately. The flux path will follow the hexagonal shape as shown in Figure 8 according to (5). When flux is in subsector I, a voltage vector that will increase the flux will be chosen. This will cause the flux locus to deviate from the circular locus. When the flux is in subsector II, a voltage vector that can reduce the flux is selected. The flux will follow the hexagonal shape as indicated by dashed arrow line in Figure 7. The selected voltage vectors produce the largest stator flux tangential components.

3.2. Modification of Flux Locus

The locus of stator flux is controlled such that it will gradually change from circular to hexagonal shape. This modification enables a smooth transition of stator voltage from PWM to six-step mode. This can be achieved by controlling the holding angle, θ_h as shown in Figure 8. Within any sector, if the angle is less

than θ_h, only one voltage vector is selected continuously and the selection is as described above. On the other hand, if the angle is larger than θ_h but less than (60°- θ_h), the flux is regulated within its hysteresis band. The shape of the flux is completely hexagonal if $\theta_h = \frac{\pi}{6}$. The holding angle is adjusted slowly to increase from 0 to $\frac{\pi}{6}$ rad to prevent overcurrent.

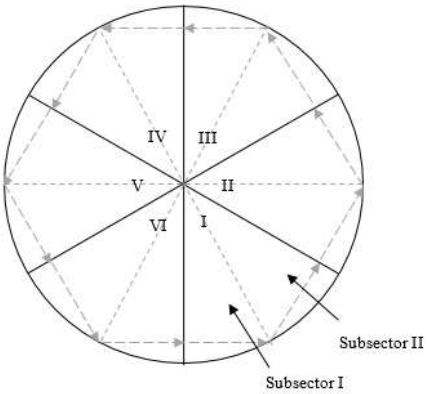

Figure 7. Flux Locus

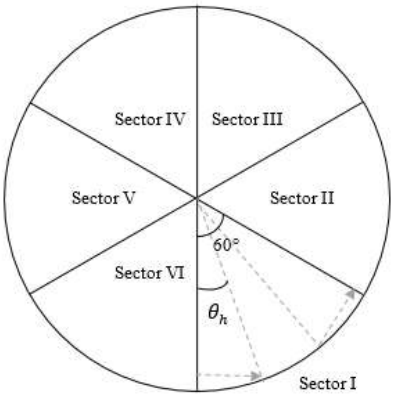

Figure 8. Holding angle, θ_h in Stator Flux Plane

The flux error status is modified as described in the flowchart as shown in Figure 9. The modified flux error status is fed into the look-up table so that the suitable voltage vectors will be chosen to either increase or decrease the flux. When $\sigma_\varphi{}^{new}$=1, the stator flux has to be increased. When $\sigma_\varphi{}^{new}$=0, it means that the stator flux has to be decreased. When the modified flux error status, $\sigma_\varphi{}^{new} = \sigma_\varphi$ the flux will increase or decrease following the normal DTC algorithm.

It is noted that the holding angle, θ_h is always $0 < \theta_h \leq 30°$. The flux locus will be in round shape when the $\theta_h = 0°$. The shape of flux locus will change gradually becoming hexagonal as the θ_h increases. The flux locus will be hexagonal in shape when the $\theta_h = 30°$. The modification of flux locus by adjusting the θ_h is shown in Figure 10.

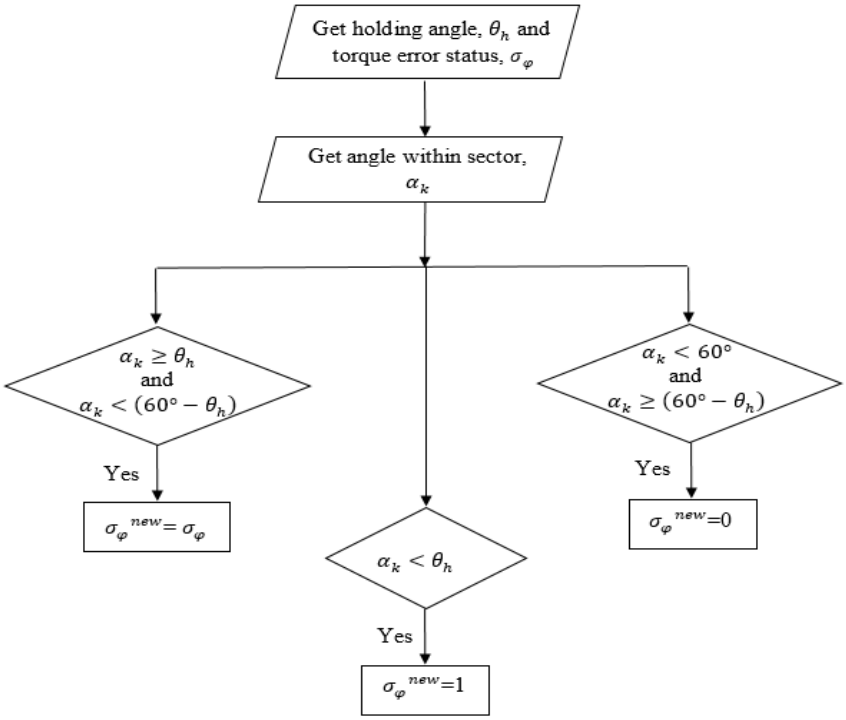

Figure 9. Flowchart of Modification of Flux Error Status, $\sigma_\varphi{}^{new}$

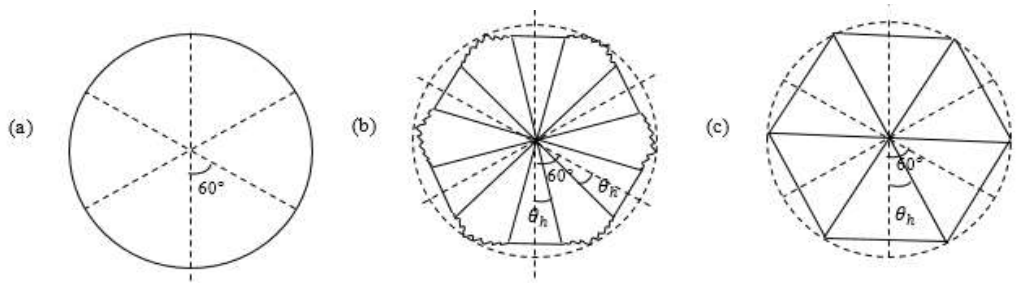

Figure 10. Flux Locus (a) $\theta_h = 0$ (b) $\theta_h = 15°$ (c) $\theta_h = 30°$

4. RESULT AND DISCUSSION

Figure 11(a) shows that in conventional DTC which is hysteresis based, the maximum speed that the motor can run is at 171 rad/s which is 1632.9 rpm. Torque starts to fail to regulate at approximately 0.85sec. When the proposed strategy is implemented, as displayed in Figure 11(b), the maximum speed that the motor can keep up to is at 195.6 rad/s which is 1867.8 rpm. This shows an increase in speed as much as 14.39%. The torque starts to fail at 1.05sec which shows an extension of constant torque region as much as 23.5%.

Figure 12 until Figure 14 show the simulation results of waveforms of torque, d-q axis components of flux vectors, changes in flux locus and phase voltages of both conventional DTC and proposed DTC at different speed. In the proposed strategy, the waveforms are simulated at different speed to obtain the desired holding angle ranged from 0° ,15° and 25°. In the simulation, at speed 105 rad/s, the holding angle is 0°. In order to obtain holding angle of 15°, the speed has to be adjusted until it reaches 141.1 rad/s. Other than that, for holding angle 25°, the speed are adjusted to 165 rad/s.

In conventional DTC, when motor speed reaches the base speed, the torque regulation is not effective. By using the proposed strategy which is setting the holding angle to 25°, the torque response is obviously improved. The d-q flux deviates from the circular locus into a hexagonal shape as the holding angle is increased slowly from 0° to 25°. Apparently, a smooth transition of stator voltage from PWM to six-step mode is achieved as shown in Figure 15 by using the proposed method and hence extending the constant torque region.

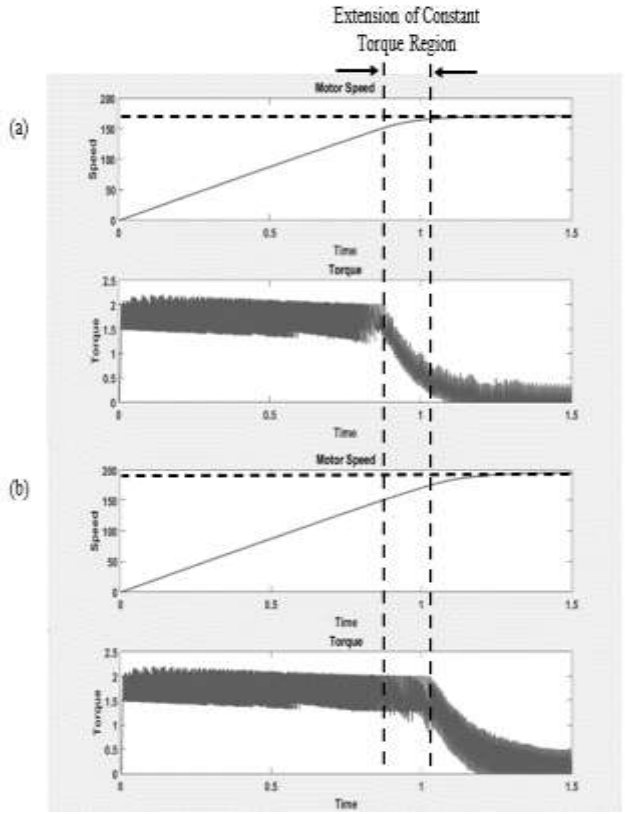

Figure 11. Comparison between (a) Conventional DTC and (b) Proposed DTC in Terms of Motor Speed and Torque

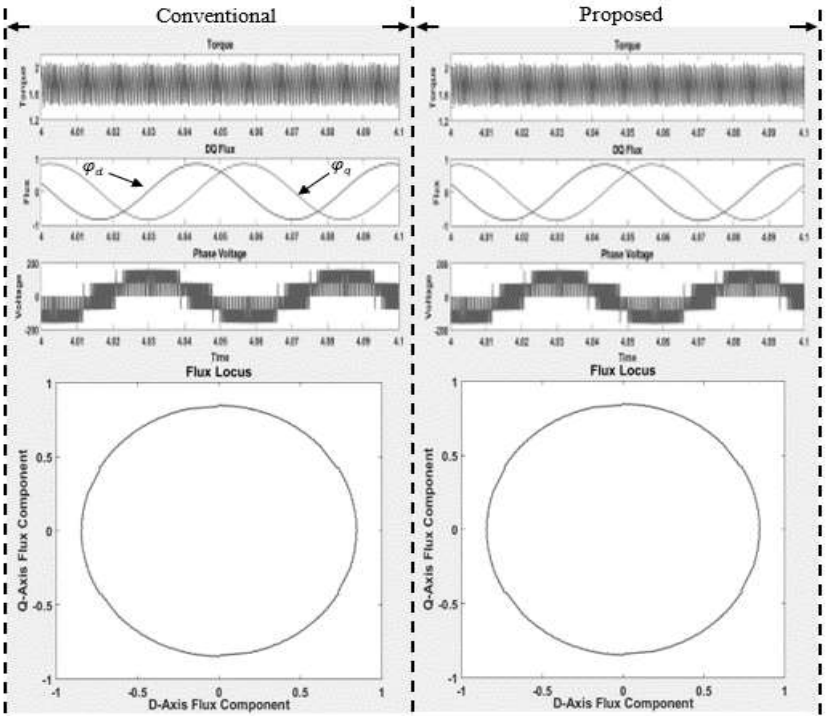

Figure 12. Waveforms Of Torque, D-Q Axis Components Of Flux Vectors, Phase Voltage and Changes In Flux Locus in Conventional DTC and Proposed DTC at $\theta_h = 0°$, $\omega = 105$ rad

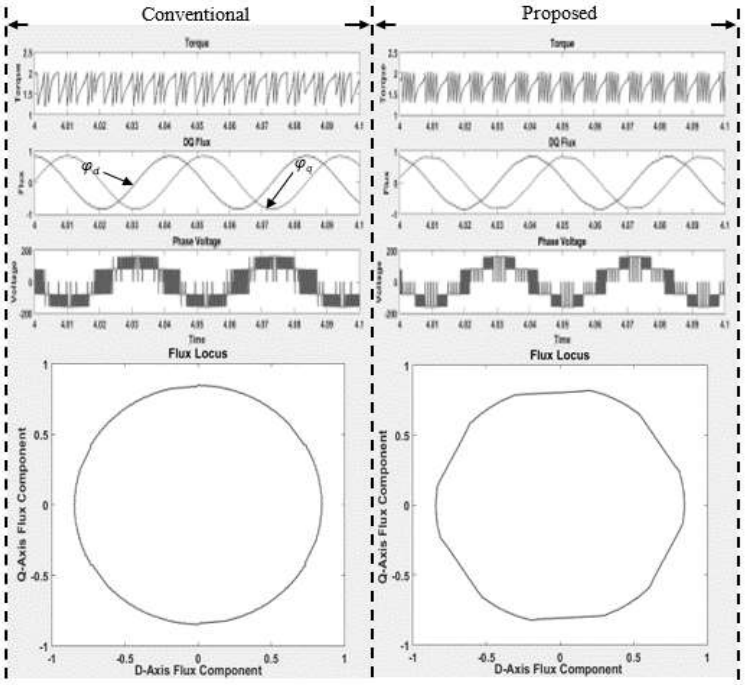

Figure 13. Waveforms Of Torque, D-Q Axis Components Of Flux Vectors, Phase Voltage and Changes In Flux Locus in Conventional DTC and Proposed DTC at $\theta_h = 15°$, $\omega = 141.1$ rad/s

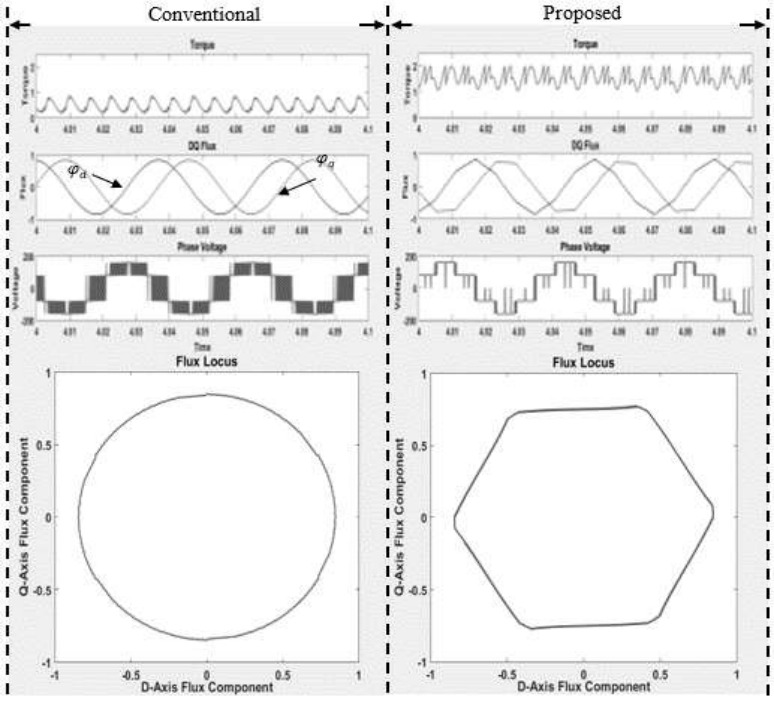

Figure 14. Waveforms Of Torque, D-Q Axis Components Of Flux Vectors, Phase Voltage and Changes In Flux Locus in Conventional DTC and Proposed DTC at $\theta_h = 25°$, $\omega = 165$ rad/s

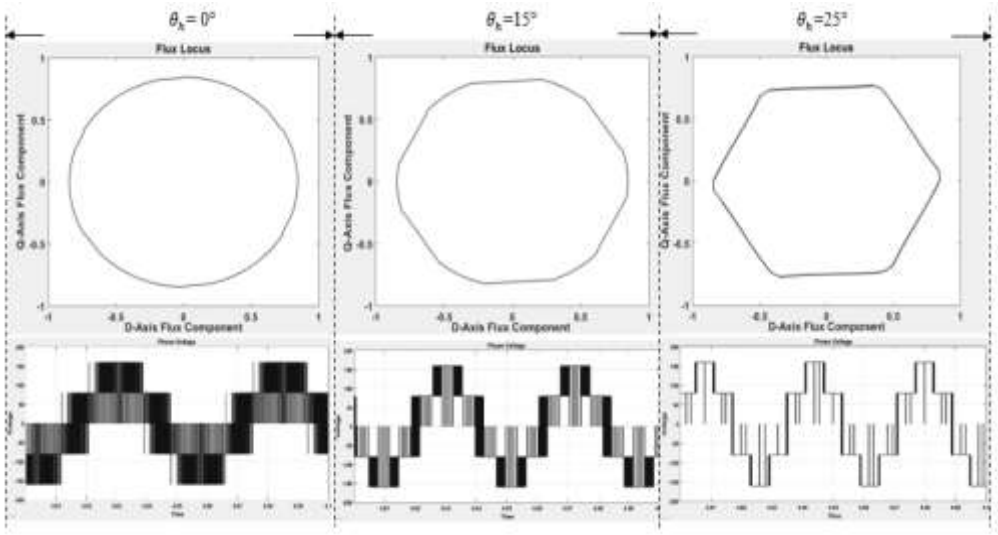

Figure 15. Transition of PWM to Six-Step using Proposed Method

From the simulation in Figure 16, the comparison of motor speed, phase voltage and the fundamental in both conventional and proposed strategy is displayed. In conventional scheme, the maximum speed that the motor can achieve is 148.2 rad/s. The torque failed to regulate at torque reference, 2Nm as the speed reaches 148.2 rad/s. When the load torque is increased, in proposed strategy, the maximum speed that the motor can achieve increased to 180.2 rad/s. In the proposed strategy, torque regulation is improved when overmodulation strategy is imposed at 0.17sec and the speed is increased to 180.2 rad/s. There is a transition of phase voltage waveform from PWM to six-step as displayed in proposed strategy.

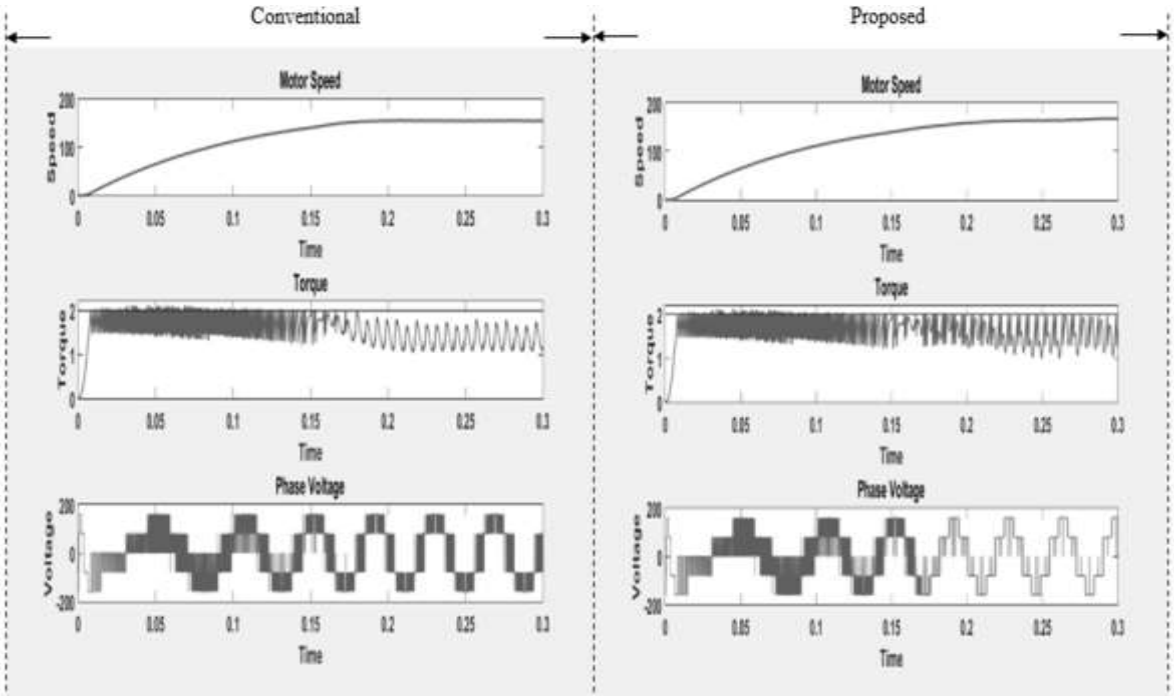

Figure 16. Comparison of Rotor Speed, Torque and Phase Voltage of Conventional and Proposed Strategy

The phase current and flux locus are observed in Figure 17. At $\theta_h = 0°$, the flux locus is in circular shape. The phase current waveform is nearly sinusoidal. As the θ_h increases, the flux locus degenerates to a

hexagon. This causes the phase current to experience increasing of distortion. The distortion is the worst as the flux locus deviates into a perfect hexagonal shape. This is a natural phenomenon which is displayed by a DTC hysteresis-based induction machine.

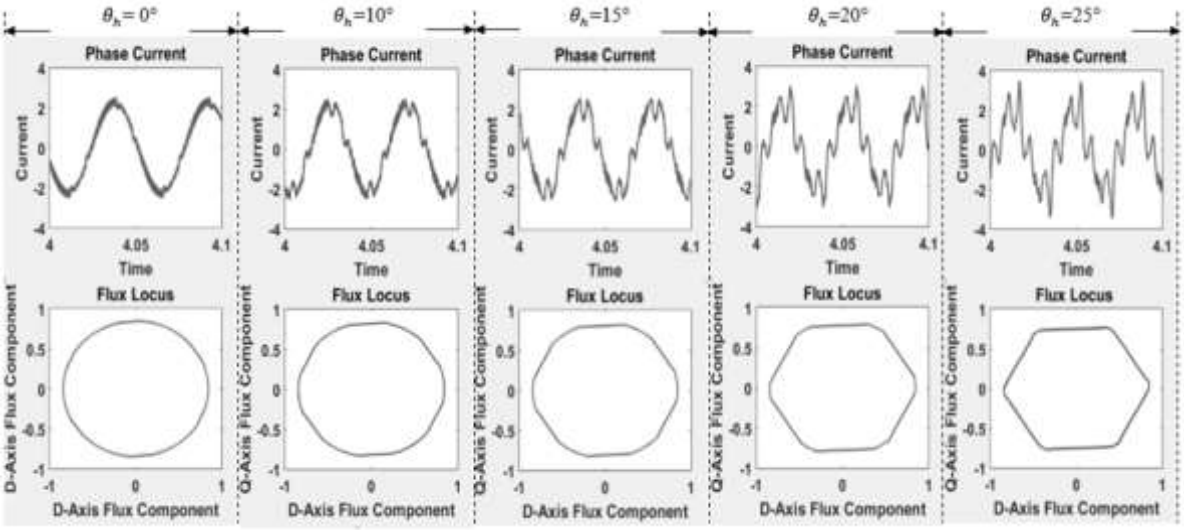

Figure17. Phase Current in Overmodulation Strategy at θ_h= 0° , 10° ,15°, 20° and 25°

5. CONCLUSION

This paper has presented dynamic performance improvement through overmodulation strategy for DTC of induction machine. The use of space vector facilitates the DTC to solve the problems in hysteresis-based DTC as well as to perform overmodulation mode. In order to retain the simplicity of the conventional DTC, the improvement on torque capability has been proposed. A simple overmodulation in DTC is performed with a slight modification on the flux error status. The aim of modifying the flux error status is to select the voltage vector which produces the largest tangential flux component to provide the fastest torque control.

Last but not least, in order to extend the constant torque region, the control of hexagonal flux locus during motor is operating in high speed condition is proposed. The circular locus will gradually change to hexagonal shape as the holding angle is adjusted slowly from 0 to $\frac{\pi}{6}$ rad. In this way, the torque capability can be improved.

REFERENCES

[1] I. Takahashi and T. Kanmachi, "Ultra-wide speed control with a quick troque response AC servo by a DSP," *Proc. EPE, Firenze (I),* vol. III, pp. 572-577, 1991.
[2] G. Buja and D. Casadei, "DTC-based strategies for induction motor drives," in *Conf. Rec. IEEE-IECON. on Power Elct*, pp. 1506-1516, 1997.
[3] T. G. Habetler, *et al.*, "Performance evaluation of a direct torque controlled drive in continous PWM-square wave transition region," *IEEE Trans. Power Electron.,* vol/issue: 10(4), pp. 464-471, 1995.
[4] S. Dangeam and V. Kinnares, "A Direct Torque Control for Three-leg Voltage Source Inverter Fed Asymmetrical Single-phase Induction Motor," 2015.
[5] I. Takahashi and T. Noguchi, "A New Quick-Response and High-Efficiency Control Strategy of an Induction Motor," *Ind. Appl. IEEE Trans.*, vol/issue: IA-22(5), pp. 820–827, 1986.
[6] M. P. Kazmierkowski and G. Buja, "Review of direct torque control methods for voltage source inverter-fed induction motors," vol. 1, pp. 981–991, 2003.
[7] P. Acarnley, "P -0.2," vol/issue: 34(4), pp. 412–414, 1998.
[8] R. N. A. Bin Raja Yunus, *et al.*, "Performance analysis of direct torque control of induction machines," *2013 Int. Conf. Electr. Mach. Syst.*, pp. 2123–2127, 2013.
[9] S. Gdaim and A. D. Torque, "Design and implementation of Direct Torque Control of Induction Machine on FPGA," 2013.